IV. RADIO ASTRONOMY*

Academic and Research Staff

Prof. A. H. Barrett
Prof. B. F. Burke
Prof. Susan G. Kleinmann
Prof. R. M. Price
Prof. D. H. Staelin
Dr. P. L. Kebabian
Dr. K. F. Kunzi
Dr. P. C. Myers
Dr. G. D. Papadopoulos
Dr. J. W. Waters
J. W. Barrett
D. C. Papa
S. J. Savatsky

Graduate Students

B. G. Anderson
K. P. Bechis
W. G. Brodsky
P. C. Crane
R. W. Freund
T. S. Giuffrida
A. D. Haschick
K-S. Lam
K-Y. Lo
R. N. Martin
R. L. Pettyjohn
R. K. L. Poon
J. H. Spencer
R. C. Walker
T. J. Warren

RESEARCH OBJECTIVES AND SUMMARY OF RESEARCH

The program in radio astronomy comprises very long baseline interferometry, in which highly stable atomic frequency standards are used to control frequency and time so as to permit the operation of radio interferometry over arbitrarily long baselines; radio spectroscopy of the interstellar medium, specifically studies of interstellar molecular emission and absorption; and the use of radio astronomical techniques to study the Earth's atmosphere.

1. Aperture Synthesis

The mapping of complex radio brightness distributions with high angular resolution can be accomplished by phase-coherent interferometric methods to synthesize apertures much larger than can be realized with single paraboloids or arrays. Complete mapping, in which the complete Fourier transform is developed, allows detailed mapping of complex distributions. Incomplete sampling of the Fourier transform plane permits more economical use of time and equipment, and our projects are concerned with both aspects.

A 3-element interferometer with 18-ft antennas on a 1000-ft baseline has been erected at the Haystack Observatory, Tyngsboro, Massachusetts. One antenna is movable over approximately 500 ft and the other two are fixed at a 500-ft spacing. Instrumentation will include 1.3 cm and 1.75 cm equipment to study the brightness distribution of strong radio sources, and the use of the interferometer system at millimeter wavelengths is being investigated.

Partial Fourier-transform experiments are being conducted with the 3-element interferometer of the National Radio Astronomy Observatory, Green Bank, West Virginia.

*This work is supported by the National Aeronautics and Space Administration (Grants NGL 22-009-016 and NGR 22-009-421, and Langley Research Center Contract NAS1-10693), the National Science Foundation (Grants GP-20769A#2 and GP-21348A#2), the Joint Services Electronics Programs (U.S. Army, U.S. Navy, and U.S. Air Force) under Contract DAAB07-71-C-0300, the U.S. Air Force -- Wright-Patterson (Contract F33615-72-C-2129), California Institute of Technology Contract 952568, the M.I.T. Sloan Fund for Basic Research (Grant 241), and the M.I.T. Thomas C. Desmond Fund.

2. Very Long Baseline Interferometry

The program of very long baseline interferometry observations continues the study of celestial H_2O masers at 1.35 cm. A joint program with the Naval Research Laboratory is aimed at establishing positions, relative motions, and time evolution of these natural masers.

3. Microwave Spectroscopy of the Interstellar Medium

Radio spectroscopy of the interstellar medium has revealed that many molecules are present in detectable amounts. In the large majority of cases the population distribution among the molecular energy levels is nonthermal, which makes it difficult to interpret the observational data in terms of physical parameters of the interstellar environment, such as temperature, gas density, radiation density, molecular composition, gas-to-dust ratio, and so forth. Our studies have focused on the emission of OH, H_2O, CH_3OH, and CH_2O in galactic HII regions and in those stellar sources that have an infrared excess. Temporal studies of OH and H_2O emission are being conducted in coordination with infrared observations of stellar sources. A program of CO observations has been initiated to study (i) emission from infrared stars and its correlation with the visual output of these stars, and (ii) emission in the galactic plane with particular emphasis on the column density of CO in the direction of x-ray sources.

4. Molecular Oxygen Emission in the Terrestrial Atmosphere

A 3-channel radiometer operating at 53.7, 54.9, and 58.8 GHz frequencies has been designed and constructed for operation in a balloon at altitudes up to ~100,000 ft. The equipment is scheduled for flight in January 1973, and will furnish data similar to that to be obtained on Nimbus-5. The atmospheric temperature profile, inferred from the microwave channels, will be compared with that from radiosondes released at the time of balloon launch.

5. Microwave Sensing of the Terrestrial Atmosphere from Satellites

The first of two 5-frequency microwave spectrometers was launched in December 1972 on Nimbus-5 and the second will follow in 1974. These experiments will determine the ability of radio-astronomy techniques near 0.5-1.3 cm wavelength to yield atmospheric temperature and moisture profiles, and give additional information about ice, snow, soil moisture, and other parameters. A third instrument is being developed to extend the temperature profile measurements to the upper stratosphere and mesosphere. A ground-based version is now yielding information about atmospheric temperatures near 30-60 km altitude and about the microwave spectrum of atmospheric O_2. An aircraft measurement program with these systems is also under way.

6. Long-Baseline Optical Interferometer

This interferometer has two 0.7 in. collecting apertures that can be separated by as much as 100 ft. When completed it should furnish information concerning angle-of-arrival fluctuations imposed by the atmosphere upon starlight, and hence information about the ultimate resolution and tracking capabilities of ground-based optical systems. The angular resolution of the system should be ~0.005 second of arc and it should yield fringes for 5^{th} magnitude stars, although with the initial system only Polaris will be observed.

A. H. Barrett, B. F. Burke, D. H. Staelin

A. RADIO OBSERVATIONS OF SCORPIUS X-1

NSF (Grant GP-21348A#2)

J. H. Spencer, G. T. Murthy
[G. T. Murthy is at the Center for Space Research, M. I. T.]

The three-element interferometer at the National Radio Astronomy Observatory at Green Bank, West Virginia, was used between May 10, 1972 and June 14, 1972, to observe 3.7 cm and 11.1 cm emission from Sco X-1. The dates and times of observation and the interferometer baselines are listed in Table IV-1. Throughout this observing program simultaneous x-ray and optical observations were made by other groups; these will be reported elsewhere. While radio data were being collected, NRAO 530 was observed for 10 minutes during each hour to determine instrumental phase stability. Flux calibration was determined from observations of 3C48, 3C286, 3C147, and 3C138. Figures IV-1 and IV-2 and the accompanying data present 25-min averages of

Table IV-1. Dates of observation and baselines.

Date (1972) and Universal Time		Local Sidereal Time	Baselines 10^2 Meter
Start	Stop		
May 10, 0210	May 10, 0910	1202 – 1900	4-15-19
May 12, 0210	May 12, 0859	1210 – 1900	3-12-15
June 9, 0010	June 9, 0830	1200 – 2030	9-18-27
June 10, 0006	June 10, 0835	1200 – 2030	9-18-27
June 11, 0002	June 11, 0830	1200 – 2030	9-18-27
June 11, 2358	June 12, 0827	1200 – 2030	9-18-27
June 12, 2354	June 13, 0822	1200 – 2030	9-18-27
June 13, 2350	June 14, 0818	1200 – 2030	9-18-27
June 14, 2346	June 15, 0814	1200 – 2030	9-18-27

two orthogonal polarizations (left-hand and right-hand circular). The rms per point is 8 m.f.u. (1 m.f.u. = 10^{-29} W m^{-2} Hz^{-1}). The agreement among the three different baselines is of the order of the relative calibration error which was 1.5 m.f.u. The fringe visibility function of the radio companions was subtracted to obtain the visibility function of the central component alone for the June 1972 data. Because data for only one day are available for each of the May 1972 baselines, it was impossible to subtract the visibility function for a standard quiet day. For this reason, in Fig. IV-1 the side companions are also included in the data, but, for our purposes, they can be assumed

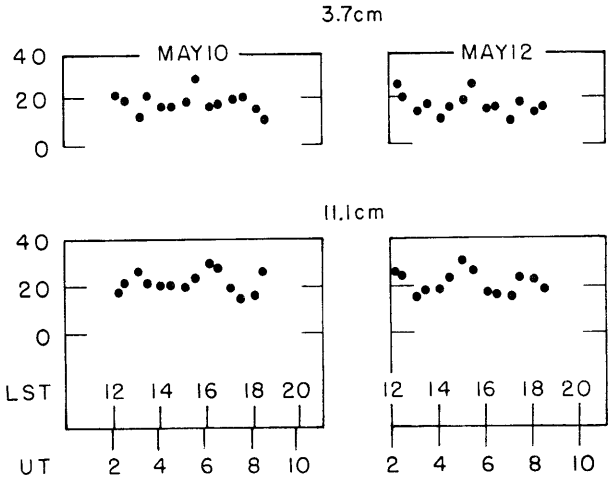

Fig. IV-1.

Flux density of the radio sources near Sco X-1 at 3.7 cm and 11.1 cm as a function of time during 2 days of observation. These data include the side companions as well as the central component. Universal time and local sidereal time at Green Bank, West Virginia, are given.

Data for Observations on May 10 and 12, 1972

UT	LST	S (11.1) (m.f.u.)	S (3.7) (m.f.u.)
		S	S
May 10, 1972			
02:21	12:13	17	22
02:46	12:38	21	20
03:19	13:12	26	13
03:45	13:37	21	22
04:20	14:13	20	17
04:45	14:38	20	17
05:20	15:13	19	19
05:45	15:38	23	29
06:20	16:13	29	17
06:45	16:38	27	18
07:20	17:13	19	20
07:45	17:38	14	21
08:19	18:13	16	16
08:44	18:38	26	11
May 12, 1972			
02:17	12:17	25	26
02:39	12:39	24	20
03:14	13:13	15	14
03:39	13:38	18	17
04:14	14:13	18	11
04:39	14:38	23	16
05:14	15:13	30	19
05:39	15:38	26	26
06:14	16:13	17	15
06:39	16:38	16	16
07:14	17:13	15	10
07:39	17:38	23	18
08:14	18:13	22	14
08:39	18:38	18	15

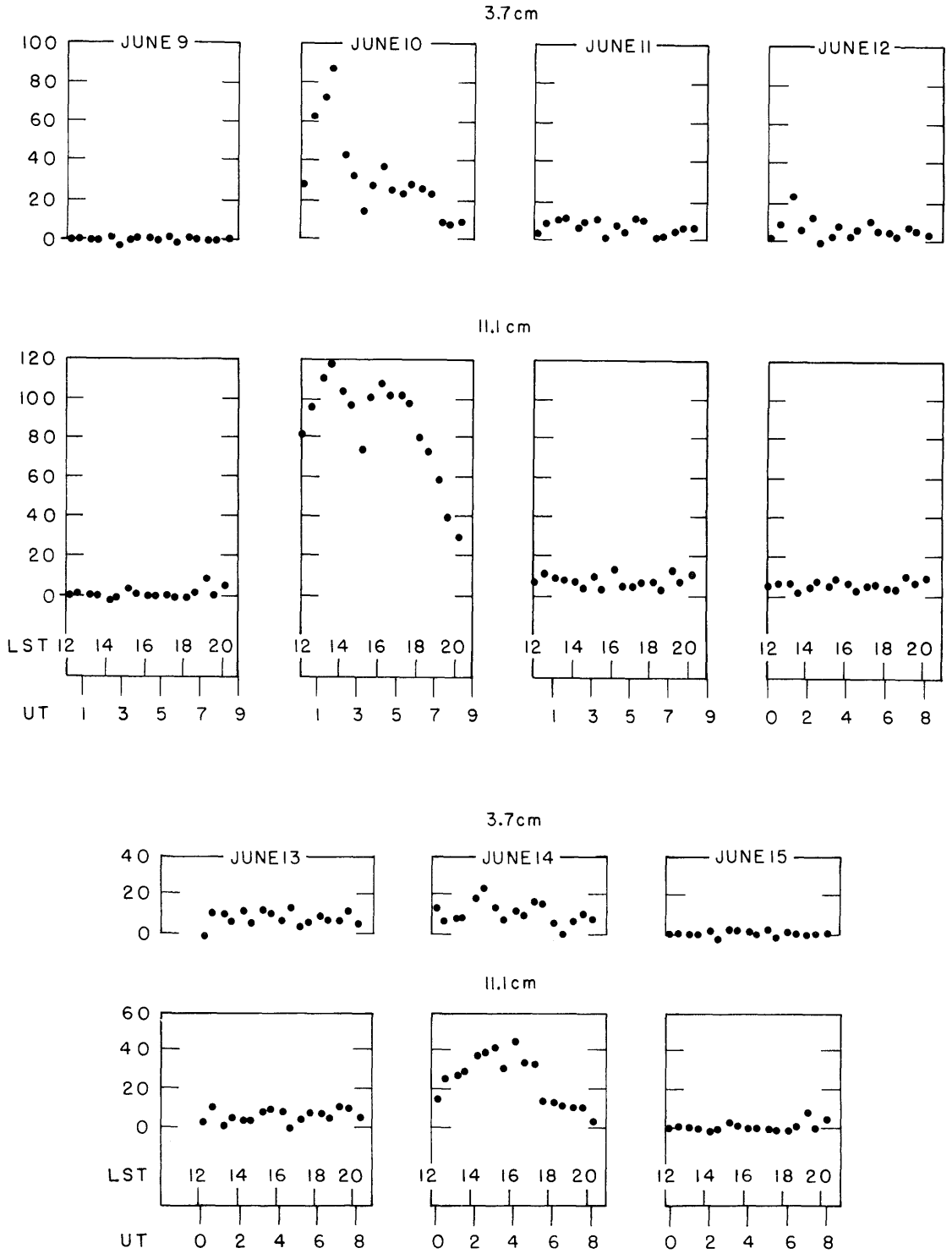

Fig. IV-2. Flux density of the central component of Sco X-1 at 3.7 cm and 11.1 cm as a function of time during 7 days of observation. Universal time and local sidereal time at Green Bank, West Virginia, are given.

Data for Observations on June 9-12, 1972

UT	LST	S (11.1) (m.f.u.)		S (3.7) (m.f.u.)		3.7 α 11.1
		S	RMS	S	RMS	
June 9, 1972						
00:20	12:11	-0.9	1.6	-0.5	1.9	
00:47	12:38	0.4	1.2	0.0	2.4	
01:22	13:13	-0.1	1.3	-0.6	3.4	
01:47	13:38	-1.2	0.8	-0.6	2.2	
02:22	14:13	-2.7	0.4	1.2	1.8	
02:47	14:38	-1.8	1.2	-2.9	1.9	
03:22	15:13	2.1	0.6	0.9	1.1	
03:47	15:38	0.2	0.8	1.6	3.0	
04:22	16:13	-1.3	0.7	1.2	3.1	
04:47	16:38	-1.1	1.9	-0.4	1.7	
05:22	17:13	-0.9	3.2	1.8	2.4	
05:47	17:38	-1.8	0.7	-1.8	1.7	
06:22	18:13	-1.8	0.6	0.9	2.2	
06:47	18:38	0.3	2.0	0.0	2.5	
07:21	19:13	7.6	4.1	-0.8	2.4	
07:46	19:38	-1.0	0.8	-0.2	1.0	
08:24	20:16	4.1	1.8	0.2	2.0	
June 10, 1972						
00:11	12:05	80.6	6.0	27.9	6.0	-0.97
00:43	12:38	95.4	6.3	62.5	17.4	-0.38
01:18	13:13	109.8	4.4	72.4	21.7	-0.38
01:43	13:38	118.6	2.1	87.5	6.3	-0.27
02:18	14:13	103.6	5.0	43.2	7.9	-0.80
02:43	14:38	96.4	1.5	32.3	3.4	-0.99
03:18	15:13	73.5	3.4	14.5	3.3	-1.52
03:43	15:38	100.7	3.8	27.6	5.9	-1.17
04:18	16:13	107.5	4.5	37.2	7.0	-0.98
04:43	16:38	101.2	5.0	25.0	11.1	-1.27
05:18	17:13	100.9	4.9	23.2	5.6	-1.34
05:43	17:38	97.5	7.5	28.3	3.7	-1.14
06:18	18:13	79.9	3.5	26.1	3.9	-1.02
06:42	18:38	73.4	5.8	23.5	5.1	-1.01
07:17	19:13	58.3	3.6	9.0	1.8	-1.70
07:42	19:38	39.6	2.1	8.4	4.9	-1.47
08:20	20:16	29.0	4.9	9.4	5.9	-1.07
June 11, 1972						
00:07	12:06	6.9	3.9	4.2	3.3	
00:39	12:38	11.4	4.4	9.4	7.8	
01:14	13:13	8.9	2.2	10.7	4.1	
01:39	13:38	8.1	3.0	11.5	4.3	
02:14	14:13	7.2	3.4	6.1	3.3	
02:39	14:38	3.6	1.5	9.7	4.6	
03:14	15:13	9.3	3.9	11.1	2.3	
03:39	15:38	3.6	2.2	1.7	1.9	
04:14	16:13	12.8	3.0	8.0	2.9	
04:39	16:38	4.5	3.2	4.5	3.1	
05:14	17:13	4.8	2.2	11.1	3.1	
05:39	17:38	6.4	2.2	10.5	2.8	
06:14	18:13	7.1	2.9	1.2	1.8	
06:39	18:38	3.2	3.3	2.1	0.7	
07:13	19:13	12.3	5.3	4.5	3.8	
07:38	19:38	7.1	4.3	6.9	4.8	
08:16	20:16	10.5	1.5	6.7	2.6	
June 12, 1972						
00:03	12:05	5.5	1.4	2.1	1.6	
00:36	12:38	7.2	2.0	8.8	1.1	
01:11	13:13	6.6	1.8	22.7	5.5	
01:35	13:38	1.9	2.1	5.8	2.8	
02:10	14:13	4.6	2.4	12.8	2.2	
02:35	14:38	8.0	4.1	-0.4	1.7	
03:10	15:13	5.7	3.0	2.4	3.8	
03:35	15:38	8.7	2.5	7.8	4.1	
04:10	16:13	6.4	3.2	2.4	3.3	
04:35	16:38	3.3	1.4	6.9	3.6	
05:10	17:13	5.6	1.7	10.6	4.7	
05:35	17:38	7.9	2.1	5.7	3.6	
06:10	18:13	4.5	4.0	4.4	4.9	
06:35	18:38	3.8	3.4	2.4	3.8	
07:10	19:13	10.2	4.7	7.6	6.0	
07:35	19:38	7.1	2.6	5.9	2.9	
08:14	20:16	8.7	2.0	3.8	3.8	

Data for Observations on June 13-15, 1972

UT	LST	S (11.1) (m.f.u.)		S (3.7) (m.f.u.)		$\alpha_{11.1}^{3.7}$
		S	RMS	S	RMS	
June 13, 1972						
00:00	12:06	3.4	1.8	-0.8	2.4	
00:32	12:38	11.2	3.5	10.5	2.3	
01:07	13:13	1.0	1.9	10.5	5.0	
01:31	13:38	5.4	3.1	6.3	4.6	
02:06	14:13	3.8	1.5	11.6	4.0	
02:31	14:38	3.7	2.1	5.1	4.3	
03:06	15:13	7.8	3.2	12.1	8.2	
03:31	15:38	8.7	3.2	10.4	3.1	
04:06	16:13	7.8	3.9	6.2	1.9	
04:31	16:38	-0.9	0.7	12.9	3.2	
05:06	17:13	4.2	3.0	2.7	4.3	
05:31	17:38	7.4	1.6	6.1	2.2	
06:06	18:13	7.3	4.1	9.4	5.8	
06:31	18:38	4.9	1.5	6.6	3.6	
07:06	19:13	10.3	3.7	6.4	2.6	
07:31	19:38	10.0	2.3	11.7	3.6	
08:06	20:16	4.7	3.4	5.1	5.0	
June 14, 1972						
00:03	12:13	14.4	3.2	13.2	4.8	-0.067
00:28	12:38	24.7	5.7	6.5	2.2	-1.3
01:03	13:13	26.7	4.9	7.8	1.8	-1.11
01:28	13:38	28.6	3.5	8.2	5.5	-1.17
02:02	14:13	37.0	3.4	17.9	2.8	-0.66
02:27	14:38	38.1	3.8	22.9	4.7	-0.46
03:02	15:13	41.2	1.7	13.3	6.0	-1.05
03:27	15:38	29.9	3.1	7.0	3.5	-1.42
04:02	16:13	44.3	4.7	10.8	2.7	-1.26
04:27	16:38	33.2	2.3	8.9	3.2	-1.09
05:02	17:13	31.5	2.2	16.1	3.5	-0.63
05:27	17:38	13.1	3.0	14.8	4.6	+0.13
06:02	18:13	13.1	3.7	4.9	3.1	-0.87
06:27	18:38	10.9	2.9	-0.5	2.2	<-1.1
07:02	19:13	10.5	4.9	6.3	4.6	-0.46
07:27	19:38	9.8	4.1	9.5	7.4	0.0
08:04	20:16	2.7	2.8	7.5	2.2	+0.9
June 15, 1972						
23:56	12:10	-0.9	1.6	-0.5	1.9	
00:24	12:38	0.4	1.2	0.0	2.4	
00:59	13:13	-0.1	1.3	-0.6	3.4	
01:24	13:38	-1.2	0.8	-0.6	2.2	
01:58	14:13	-2.7	0.4	1.2	1.8	
02:23	14:38	-1.8	1.2	-2.9	1.9	
02:58	15:13	2.1	0.6	0.9	1.1	
03:23	15:38	0.2	0.8	1.6	3.0	
03:58	16:13	-1.3	0.7	1.2	3.1	
04:23	16:38	-1.1	1.9	-0.4	1.7	
04:58	17:13	-0.9	3.2	1.8	2.4	
05:23	17:38	-1.8	0.7	-1.8	1.7	
05:58	18:13	-1.8	0.6	0.9	2.2	
06:23	18:38	0.3	2.0	-0.0	2.5	
06:58	19:13	7.6	4.1	-0.8	2.4	
07:23	19:38	-1.0	0.8	-0.2	1.0	
08:01	20:16	4.1	1.8	0.2	2.0	

to have no time variability.

Several things are very significant in these results. The most obvious is the presence of two major flares, one of which is double. This indicates a frequency of major flaring very close to the figure of 15% reported by Wade and Hjellming.[1, 2] We did not find any further evidence of the sawtooth variability reported by Wade and Hjellming. The other patterns seem to represent approximately the same percentages of occurrence as previously reported.

The spectral index of the double flare on June 10, 1972 is very interesting (see Fig. IV-3). For the first flare the spectral index α (where $S = \nu^{\alpha}$) was -1.0 when the observing session began. As the intensity of the flare increased the spectral index flattened to -0.4 until after the peak. Then it steepened again to -1.5 when the second flare clearly dominated. The second flare on June 10, 1972 may be confused with the aftereffects of the first flare, but the apparent spectral index is near -1.2 throughout the whole event. The spectral index for the weak flare of June 14, 1972 shows more variation. Some of this may be the result of the lower signal level, but it is clear that the spectral index did not become flat as it did in the first flare of June 10, 1972. This event seems much more closely related to the second flare of June 10, 1972. Note the positive spectral index in the decay.

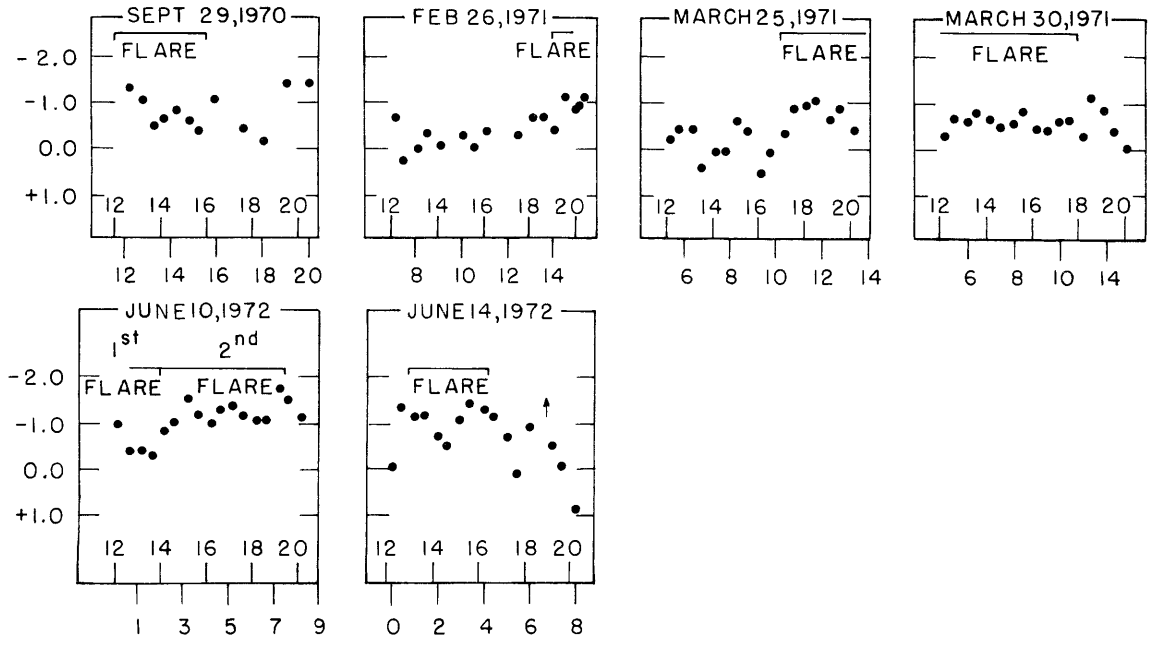

Fig. IV-3. Spectral index of Sco X-1 on days when the flux at 11.1 cm exceeded 40 m.f.u. and for which 3.7 cm data exist. Data from Hjellming and Wade[1, 2] are included with the June 10, 1972 and June 14, 1972 data reported here.

More evidence of the flare behavior of Sco X-1 can be found in the data of Hjellming and Wade. Figure IV-3 includes the spectral index for each of their flare days. The flare of September 29, 1970, had a spectral index of -1.4 at the beginning of the observing period. At the peak, the spectral index decreased to -0.5. Hjellming and Wade conclude that the spectral index is usually near -0.5. The flares on March 30, 1971, and the first flare on June 10, 1972, followed this same pattern. The flares of February 26, 1971, March 25, 1971, and June 14, 1972, however, seem to have a spectral index closer to -1.0 or -1.5 than to -0.5. The second flare on June 10, 1972 may be confused with the aftereffects of the first flare on that date, but the apparent spectral index is near -1.2. It is interesting to note that the spectral indices on February 26, 1971, March 25, 1971, and June 14, 1972, are steepest during the flare periods. It appears to us that there may be two types of flare, one with a spectral index near -0.5 and the other with a spectral index near -1.5. The evidence for this behavior is not strong because even when Sco X-1 is not flaring the spectral index varies more than noise analysis indicates it should.

The authors would like to thank R. M. Hjellming for stimulating discussions and the use of his visibility function subtraction program.

References

1. R. M. Hjellming and C. M. Wade, "The Radio Sources Associated with Scorpius X-1," Astrophys. J. 164, L1 (1971).
2. C. M. Wade and R. M. Hjellming, "Further Radio Observations of Scorpius X-1," Astrophys. J. 170, 523-528 (1971).

B. CONTINUUM RADIO STRUCTURE OF THE GALACTIC DISK

NSF (Grant GP-21348A#2)

R. M. Price

For the purposes of structure studies, the continuum radio emission in the disk of our galaxy can be divided into three categories. First, there is a contribution from the general disk of the galactic plane; second, a component associated with large-scale spiral features in the disk; and finally, discrete sources. In this study we are concerned mainly with the first two.

The general distribution of the base disk radio component was discussed earlier[1] and it was determined that the base disk did not have a constant volume emissivity but probably varied as a function of distance from the center of the galaxy. Further study has shown that a volume emissivity function of the form $e^{-\alpha R}$ yields a good fit to the observed data. R is the distance from the center of the galaxy, and α is a scale factor

associated with the effective radius of the galactic continuum disk.

In 1959, Mills[2] suggested that the bumps or steps in the observed brightness profile along the galactic plane are associated with spiral features in the disk. With the subsequent development of the Density Wave theory,[3] we now have a basis for presenting models to explain the radio continuum from the spiral features.

Figure IV-4 shows a model used in the present study. The basic spiral pattern is

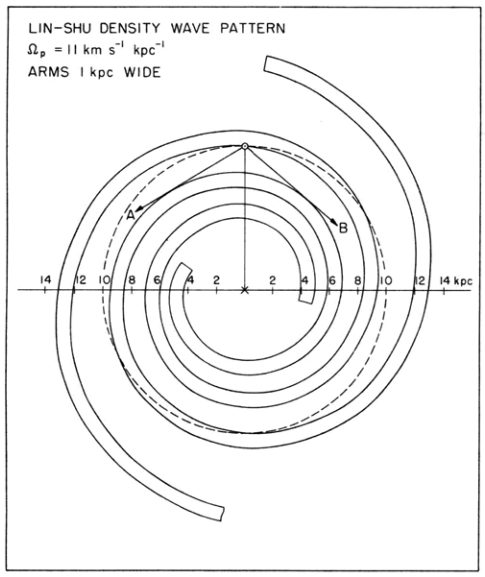

Fig. IV-4.
Continuum radio spiral arm model based on the spiral pattern of Lin and Shu.[3] Arms have constant (1 kpc) width. (Ωp = 11 km s^{-1} kpc^{-1}.)

taken from Lin and Shu.[3] For present purposes, we assumed that the spiral features are continuous and of constant (1 kpc) width, and that the density wave strength is constant over the disk. (The strength of the density wave affects the amount of compression in the spiral features and hence the relative volume emissivity.) In fitting such a model to the observed brightness temperatures a prime parameter affecting the longitudes at which changes in brightness occur is the position of the sun with respect to the spiral features. The longitudes at which the brightness temperatures increase greatly can be expected to coincide with tangential points A and B of the spiral feature just interior to the sun, as shown in Fig. IV-4. Interior features will show up as additional bumps or increases on the brightness temperature along the galactic plane.

The results of using this model are shown in Fig. IV-5. The dashed line shows the

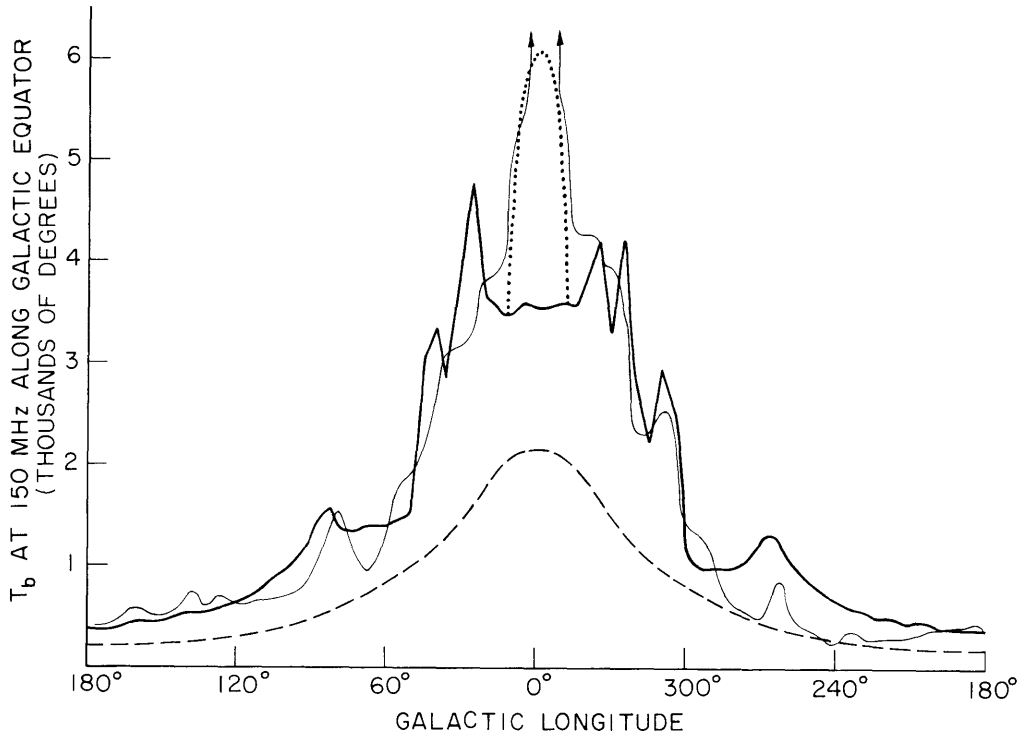

Fig. IV-5. Comparison of observed and model brightness temperatures along the galactic plane. Dashed line: contribution from base disk. Heavy solid line: calculated contribution from both disk and spiral features. Dotted line: additional contribution from a uniform nonthermal disk with 2-kpc radius located at the galactic center. Light line: observed brightness temperature along the galactic equator at 150 MHz.[4]

brightness temperature attributable to the base disk with an effective radius of ~16 kpc. The heavy solid line gives the total brightness (both disk and spiral features) obtained from the simple density wave model shown in Fig. IV-4.

The lack of total agreement of observations with such a simple model is not surprising, since we know from studies of external galaxies that spiral features are seldom smooth and continuous over the entire disk in galaxies. For instance, the small bumps in the brightness distribution at longitude 55° and 295° might well be due to Carina-type features such as those discussed by Bok, Hine, and Miller.[5]

In the present model the ratios of brightness temperatures along the plane that are attributable to the disk and spiral features vary from 1:1 near the anticenter to approximately 2:1 in some regions within 60° of the galactic center. This corresponds to differences in volume emissivity of approximately four between disk and arm regions.

The fit of this simple model is far from precise. The general agreement, however, indicates that with this approach light can be shed on matters such as relative radio

emission from the arms and general disk regions, the general form of the spiral pattern (as originally suggested by Mills[2]), and the position of the sun with respect to local spiral features.

References

1. R. M. Price, Quarterly Progress Report No. 104, Research Laboratory of Electronics, M.I.T., January 15, 1972, p. 80.
2. B. Y. Mills, in R. N. Bracewell (Ed.), Proc. Paris Symposium on Radio Astronomy (Stanford University Press, Stanford, California, 1959), p. 431.
3. C. C. Lin and F. H. Shu, in H. van Woerden (Ed.), Proc. IAU Symposium No. 31 (Academic Press, Inc., London, 1967), p. 313.
4. T. Landecker, Private communication, 1972.
5. B. J. Bok, A. A. Hine, and E. W. Miller, in W. Becker and G. Contopoulos (Eds.), Proc. IAU Symposium No. 38 (D. Reidel Publishing Co., Dordrecht, The Netherlands, 1970), p. 246.

C. M.I.T. THREE-ELEMENT INTERFEROMETER

NSF (Grant GP-21348A#2)

G. Papadopoulos, B. F. Burke, D. C. Papa,
R. M. Price, J. W. Barrett

We are integrating the components of a new M.I.T. radio interferometer, which has been built near the Haystack Observatory, at Tyngsboro, Massachusetts. This system is an extension of the 2-element pilot project that was completed in 1970. It has three 18-ft radio antennas on an E-W baseline, which were installed on November 20, 1972. Two of the antennas are fixed at a distance of 500 ft and the third will be movable on a maximum 1000-ft baseline. The resolution attained with this baseline at 22 GHz will be 9 seconds of arc.

The parabolic reflectors are placed on azimuth-elevation mounts. The reasons for having picked az-el rather than polar mounts are that they give a full range of hour-angle coverage and better pointing accuracy. The rms surface deviation of the parabolic surfaces is less than $0.''015$ and will permit operation of the system at 3-mm wavelength. This is a particularly significant wavelength because of the CO molecular emission that has been discovered in many galactic clouds.

The E-W baseline was chosen because a better coverage of the transform plane can be obtained with this orientation. The E-W orientation has also been adopted for two other supersynthesis radio interferometers operating in Cambridge, England, and Westerbork, in the Netherlands. Thus it will be possible to compare the brightness temperature maps obtained with the M.I.T. interferometer and those derived from the

other systems that operate at lower frequencies (6-cm wavelength).

At first, the system will be used at 22.235 GHz at which frequency there are galactic regions emitting strong H_2O line radiation which can be used as calibrators. We are now building the radiometers which are expected to have a noise temperature of approximately 1000°K. The local oscillator will be constructed by doubling the output of an X-band oscillator which is phase-locked by means of a phase-lock system built at M.I.T.

A small computer (NOVA 820) with a Linc tape system is incorporated in the system design. The computer will point the antennas, change the compensation delays, and do a real-time least-squares fit on the data. The software and hardware for the control system are 60% complete.

D. 21-CENTIMETER VLBI OBSERVATIONS OF PULSARS

NSF (Grant 21348A#2)

P. C. Crane, G. D. Papadopoulos

A group of observers from the Massachusetts Institute of Technology and the California Institute of Technology has performed very long baseline interferometric (VLBI) continuum observations of pulsars at 21 cm. These are the first-epoch observations in a program to search for apparent motions of pulsars.

1. System and Data Reduction

The observations were made, June 2-6, 1972, with the 3-element interferometer of the National Radio Astronomy Observatory (the choice of frequency was determined by the availability of the 21-cm system at NRAO) and with the 2-element interferometer and the 130-ft radio telescope of the California Institute of Technology Owens Valley Radio Observatory, Bishop, California. Two antennas at each site were continually tracking quasi-stellar sources while a third tracked a pulsar; this technique is designed to provide continuous monitoring of the phases of our sources. The data were recorded at each site by the Mark II VLB video recording system.[1] The records gave alternate 1-s signals from the quasi-stellar sources interspersed with short (~50 ms) records of each pulsar pulse. The data tapes were then transported to NRAO, in Charlottesville, Virginia, where preliminary reduction was completed late in September 1972, with the use of modified programs for the Mark II VLB processor.[1]

2. Results

The pulsars that were observed were chosen on the basis of nearness inferred from 3 independent (and often conflicting) criteria: (i) observed signal strength, (ii) dispersion measure[2] (from the time delay vs frequency of the pulses which gives the

integrated electron density to the pulsar), and (iii) neutral hydrogen absorption[3] (which gives the integral of n_H/T to the pulsar). We obtain distance estimates from (ii) and (iii) by making simplifying assumptions about the uniformity of n_e, n_H, and T. Because of the deduced proximity of the pulsars, both parallax and random velocities should cause apparent motions with respect to the fixed quasi-stellar sources used as calibrators, which should be detectable with the $0.''01$ resolution of our observations.

In the preliminary reduction, we obtained fringes on all of our calibration sources and on one pulsar, which was 0329+54. We shall continue our data reduction and have requested additional observing time before next spring for second-epoch observations.

The principal investigator for this program is Dr. M. S. Ewing of the California Institute of Technology.

References

1. B. G. Clark, R. Weimer, and S. Weinreb, Electronics Division Internal Report 118, National Radio Astronomy Observatory,1972.
2. M. I. Large, in R. D. Davies and F. G. Smith (Eds.), The Crab Nebula (Springer Verlag New York, Inc., New York, 1971), p. 165.
3. C. P. Gordon, K. J. Gordon, and A. M. Shalloway, Nature 222, 129 (1969).

E. NEW H_2O SOURCES ASSOCIATED WITH INFRARED STARS

NSF (Grant GP-20769A#2)

A. H. Barrett, K. P. Bechis

1. Introduction

Early work on 1.35-cm water-vapor emission from infrared stars resulted in the detection of 10 sources, all associated with variable stars (cf. Schwartz and Barrett,[1] Knowles et al.,[2] Turner et al.[3]). With one exception (NML Cyg), all had negative K-magnitudes. Since many stars searched were similar late M-type variables, this suggests that the H_2O-IR stars are relatively nearby; consequently, we examined all stars from the California Institute of Technology two-micron survey (Neugebauer and Leighton[4]) with a recorded K-magnitude less than zero. As a result, we found 3 new H_2O sources associated with stars with negative K-magnitudes, 3 others with K-magnitudes between zero and one, and one with the unusually dim K-magnitude (for this type of object) of 1.6. In view of the preponderance of negative K-magnitudes searched, and the fact that 4 positive K-magnitude H_2O-IR stars were detected, it would appear that the proximity of the IR stars to us is not a very strong criterion for finding H_2O emission. Wilson and Barrett[5] reach the similar conclusion regarding OH emission that there is no apparent correlation with K-magnitude.

Our observations were made from Fall 1971, through Fall 1972, with the 120-ft radio telescope of the Massachusetts Institute of Technology Haystack Observatory in Tyngsboro, Massachusetts.

2. Results

Table IV-2 summarizes pertinent properties of 18 stars that show H_2O emission, and Table IV-3 summarizes our new detections in more detail. All known H_2O sources are OH emitters except for RX Boo and possibly IRC-30182 (R Peg and RU Hya have not yet been observed for OH emission, but it seems fairly likely that OH emission will be found in these stars). Velocities in Table IV-2 and Fig. IV-6 are heliocentric to facilitate comparison with optical data. All other velocities listed in figures and text are with respect to the local standard of rest to facilitate comparison with radio data.

H_2O sources associated with IR stars appear to have certain common properties.

(i) All are spectral class M stars. This may be partially a selection effect as only limited searches have been made in other spectral classes. In our survey we used as a guide the CALTECH two-micron survey which would bias us generally toward class M stars. Only about half of the stars that we observed, however, are late M-type, typically M6 to M8. Nevertheless, a striking fact is that 14 of 18 H_2O-IR stars whose spectral class is known are specifically of late M-type. Of the remaining four, two

Table IV-2. Properties of 18 stars showing H_2O emission.

Star	IRC	Class	Period (days)	Type	K	I-K	Heliocentric Velocities (km/sec)					Add for Conversion to L. S. R. (km/sec)
							OH		H_2O	Optical		
							low	high		em	abs	
New Stellar H_2O Sources												
NML Tau	10050	M8e	532		-1.2	6.8	29.6	62.9	31-37	41	63	-12.3
RR Aql	00458	M7e	394	M	0.7	4.7	8.2	17.4	13	1	15	14.9
R Crt	-20222	M8	160	SR	-1.2	4.8	10	(30)	21-27			-7.6
	-30182	M4			-0.3	2.9	—	—	26			-5.5
R Peg	+10527	M7ev	378	M	0.3	4.3			30	6	20	-6.0
	-20424	—			0.9	6.3	-12	6	6			12.8
RU Hya	-30215	M6e	334	M	1.56	3.8			0	-11	3	-3.2
Previously Known Stellar H_2O Sources												
VY CMa	-30087	M3e	Irr		-0.7	5.6	13	64	35	14, 54	49, 63	-19.0
NML Cyg	40448	M			0.6	8.2	-40	5	-25		7	16.5
VX Sgr	-20431	M4e	688	SR	-0.4	4.7	-26	13	-10	-34 to -22	12	12.2
R Aql	10406	M7e	300	M	-0.6	5.0	24	36	31	21	32	18.0
U Her	20298	M7e	406	M	-0.3	4.2	-41	27	-33	-45	28	18.1
W Hya	-30207	M8e	382	SR	—	—	35	45	40	28	42	2.0
S CrB	30272	M7e	361	M	-0.2	3.9	-21	-10	-13	-21	1	16.4
U Ori	20127	M8e	372	M	-0.5	5.4	-29.5	-22.7	-24	-34	-21	-12.8
RX Boo	30257	M8e	78	SR	-1.9	4.6	—	—	-8.3	-18	-10	13.3
R Cas	50484	M7e	431	M	-1.8	4.9	9	25	18	10	26	8.1
R Hor?		M6ev	403	M			44	47	?	46	56	-11.0

Table IV-3. Summary of new H_2O-IR stars.

Source	Position (1950)						Notes	Peak Unpolarized[a] Flux Density (S_o) (f.u.)				Integrated Unpolarized[a] Flux ($\int S_o d\nu$) (f.u. × Hz × 10^4)[b]			
								H_2O	OH			H_2O	OH		
	h	m	s	°	'	"		22235 (MHz)	1612 (MHz)	1665 (MHz)	1667 (MHz)	22235 (MHz)	1612 (MHz)	1665 (MHz)	1667 (MHz)
NML Tau	03	50	46	+11	15	42	1,2,3,4, 5,7	60	2	—	2	2300	5	—	3
R Crt	10	58	09	-18	03	36	1,2,3,4, 5,7	250	2	—	2	3300	4	—	4
IRC-30182	11	46	13	-26	28	48	2,3,4,7?	50	—	—	1?	3000	—	—	2?
RU Hya	14	08	42	-28	38	24	4	120				2300			
IRC-20424	18	00	58	-20	19	12	4,5,7	120	2	10	15	1800	1	5	8
RR Aql	19	54	58	-02	01	12	1,2,3,4, 5,7	30	5	1	2	600	6	1	2
R Peg	23	04	08	+10	16	22	3,4,5,6	70				600			

Notes. [a]Average values, in all cases with time variations present. Also, the unpolarized H_2O values entail the assumption that preliminary measurements showing that the radiation is unpolarized are accurate.

[b]1 f.u. × Hz × 10^4 = 10^{-22} W × m^{-2}.

1. Observed in Fall 1971.
2. Observed in Winter 1971-1972.
3. Observed in Spring 1972.
4. Observed in Summer 1972.
5. Previously searched for H_2O emission by Schwartz[6]; no emission greater than 15-20 f.u. was detected over the velocity range ±100 km/sec with respect to L.S.R.
6. Previously searched for OH emission by Wilson,[5] and Wilson and Barrett[7]; no emission greater than 0.6 f.u. was detected.
7. Known OH emission source.

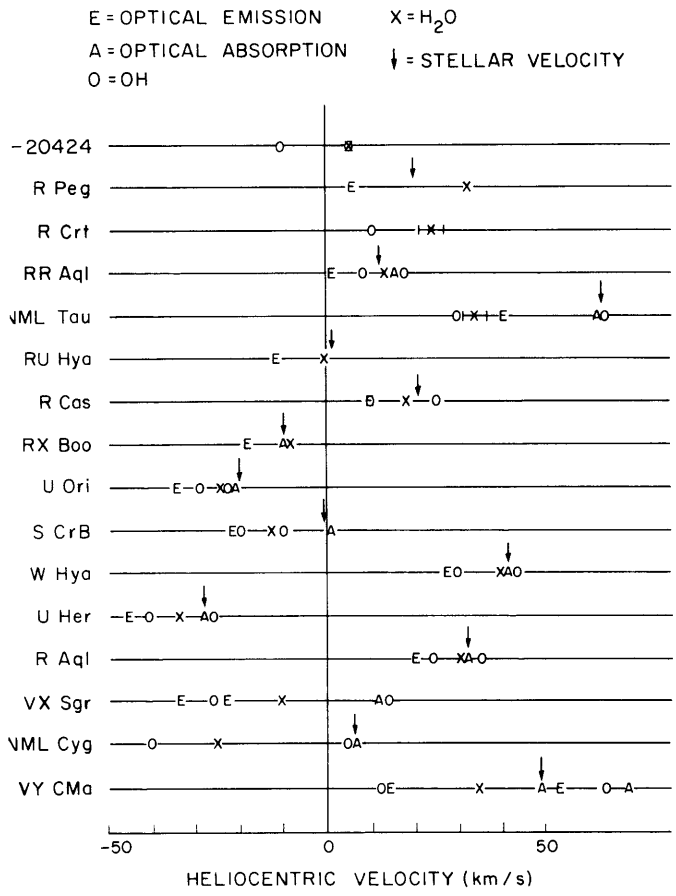

Fig. IV-6. Heliocentric velocities of various components in the optical and microwave spectra of the stellar H_2O sources.

supergiants, VX Sgr and VY CMa, are M4e and M3e; and the questionable source IRC-30182 is M4.

(ii) All are OH emission sources except RX Boo (IRC-30182 is questionable, and R Peg and RU Hya have not been examined yet). RX Boo, a relatively strong stellar H_2O emitter, has shown no OH emission stronger than 0.5 f.u., even though searches have been made numerous times at all four ground-state OH frequencies, including observations late in May 1972, when the H_2O emission brightened quite dramatically for a short time.

(iii) Sixteen of 18 H_2O sources are known variable stars at visual or infrared wavelengths. Nine of 18 stars are known Mira variables, 4 are semiregular, and one irregular (VY CMa). Two of the stars that are visible only in the infrared (NML Tau and IRC-20424) are also variable. All of these 18 stars, however, show time changes in the microwave water-vapor line, either in peak flux or total integrated flux. We have monitored some of these stars and find evidence for a correlation among optical,

infrared, and microwave intensity variations. (This is a continuing program and will be reported on in detail later.) This suggests that the H_2O maser in these sources is most probably pumped via an infrared transition. A similar conclusion has been reached regarding OH emission in infrared stars where the maser excitation is probably via the first vibrational transition at ~2.8 μ (Litvak and Dickinson[8]).

(iv) The velocity of the water-vapor emission falls between the two OH velocities and, in the majority of sources, between the optical emission and the absorption lines. Figure IV-6 shows heliocentric velocities for these components in the known H_2O-IR stars.

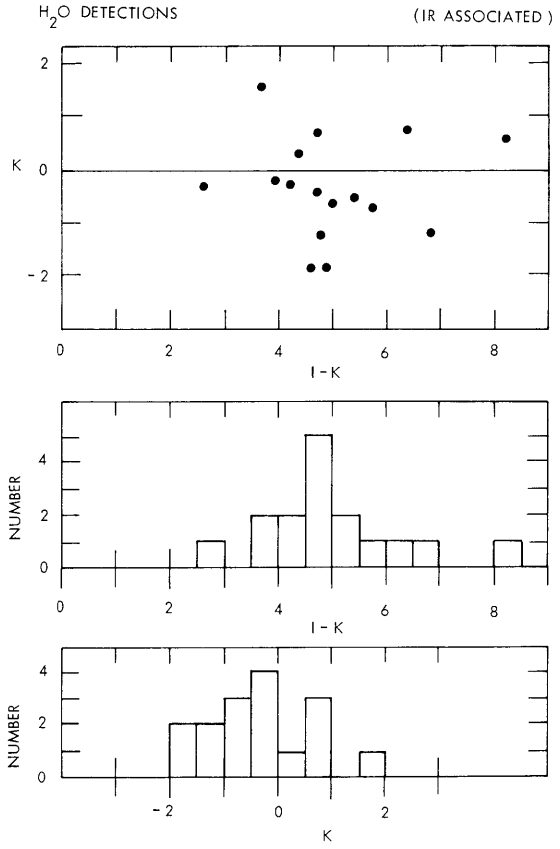

Fig. IV-7. Histograms of the distribution of the stellar H_2O sources over their I-K and K values.

(v) With the exception of the questionable water-vapor source IRC-30182, the I-K value of all H_2O sources is greater than 3.8. Indeed S CrB (I-K = 3.9) shows variability in its I-magnitude and RU Hya (I-K = 3.8) has a questionable I-magnitude. Thus we may take 4.0 as a nominal lower limit for the I-K value for a star to be an H_2O source. Figure IV-7 shows a histogram of all H_2O detections in IR stars, with a marked

clustering around I-K = 5. The average I-K for the H_2O sources is 5.1 compared with 5.9 for all OH-IR sources.

The work reported here was conducted in collaboration with Dr. Dale F. Dickinson of the Smithsonian Astrophysical Observatory, and will appear in the March 15, 1973 issue of The Astrophysical Journal.

References

1. P. R. Schwartz and A. H. Barrett Astrophys. J. 159, L123 (1970).
2. S. H. Knowles, C. H. Mayer, A. C. Cheung, D. M. Rank, and C. H. Townes, Science 163, 1055 (1969).
3. B. E. Turner, D. Buhl, E. B. Churchwell, P. G. Mezger, and L. E. Snyder, Astron. Astrophys. 4, 165 (1970).
4. G. Neugebauer and R. B. Leighton, Two-Micron Sky Survey, A Preliminary Catalog (National Aeronautics and Space Administration, Washington, D. C., 1969).
5. W. J. Wilson, Ph. D. Thesis, Department of Electrical Engineering, M. I. T., 1970.
6. P. R. Schwartz, Ph. D. Thesis, Department of Physics, M. I. T., 1971.
7. W. J. Wilson and A. H. Barrett, Astron. Astrophys. 17, 385 (1972).
8. M. M. Litvak and D. F. Dickinson, Astrophys. Letters (in press).

F. OBSERVATIONS OF HIGH-J ATMOSPHERIC O_2 LINES AT ARECIBO OBSERVATORY

NASA (Contract NAS1-10693)

J. W. Waters

The 53 GHz radiometer system constructed for sensing upper stratospheric temperatures[1] was taken to Arecibo Observatory (Puerto Rico) in October, 1972, and measurements were made of atmospheric emission from the five high-J O_2 lines reported earlier.[2] The purpose of the measurements from Arecibo was to observe the predicted narrowing of the lines (because of less separation of the Zeeman components) in the weaker magnetic field at Arecibo, and to look for the slight linear polarization in the

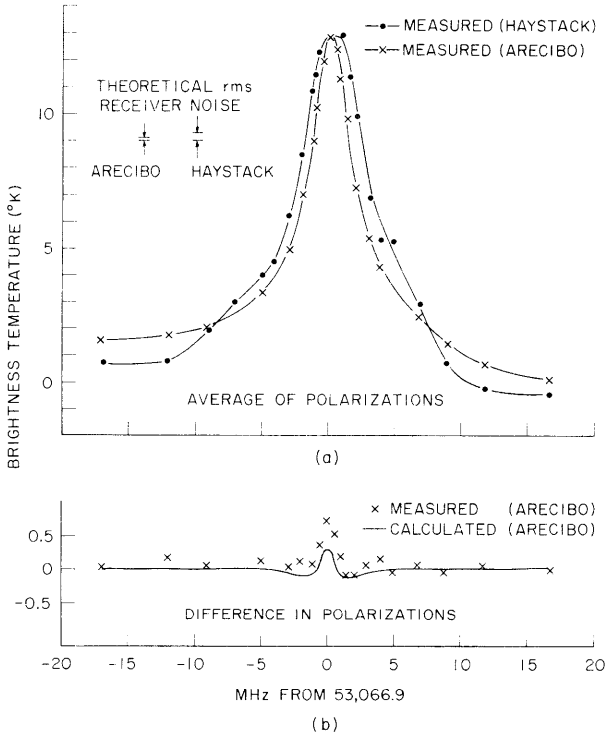

Fig. IV-8. (a) Atmospheric zenith emission by the 27_- O_2 line as measured on August 30, 1972 from Haystack Observatory (magnetic latitude 55°) and on November 1, 1972 from Arecibo Observatory (magnetic latitude 29°). The Haystack measurement is noisier because it represents a shorter integration time than the Arecibo measurement.

(b) Measured and calculated electric polarization of the 27_- O_2 line for Arecibo. The linear polarization in the magnetic east-west direction is stronger than that in the magnetic north-south direction.

emission from the lines expected at low magnetic latitudes.

Figure IV-8 shows measurements of the 27_ line made at Arecibo with the filter system.[1] For comparison, the line measured at Haystack is also shown. The Arecibo line is narrower than the Haystack line by approximately the expected amount, although both lines are stronger than calculated. The difference in the two linear polarizations observed at Arecibo is also given in Fig. IV-8 and is larger than calculated by approximately the same amount as the amplitudes. The two linear polarizations were observed by rotating the radiometer so that the linearly polarized horn antenna produced a measured electric field which was alternately parallel and perpendicular to the terrestrial magnetic field. The direction of the magnetic field was taken to be that at the surface measured by a simple hand compass. The switching period between the two polarizations was 10 min. The calculated polarization difference shown in Fig. IV-8 assumed a magnetic latitude of 29° and a 15°N annual average temperature model, corresponding to conditions at Arecibo. Higher resolution measurements were also made

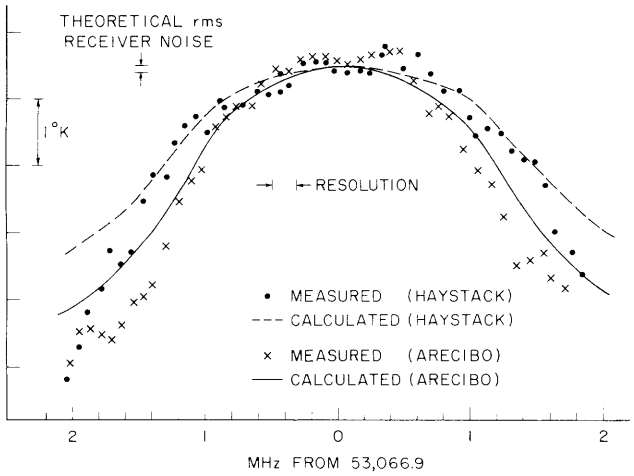

Fig. IV-9.

High-resolution measurements of the 27_ O_2 line atmospheric zenith emission made with the Haystack and Arecibo correlators on August 30 and November 1, 1972, respectively. The measurements are the average of two orthogonal linear polarizations. Calculations which linearly sum the absorption by the various O_2 lines are also given.

of the 27_ line with the Arecibo autocorrelation, and the results are compared with the Haystack autocorrelator measurements in Fig. IV-9. The correlator measurements at Arecibo were made with the assistance of Dr. Alan Parrish of the Arecibo Observatory staff.

References

1. J. W. Waters, R. M. Paroskie, J. W. Barrett, D. C. Papa, and D. H. Staelin, "Radiometer System for Ground-Based Measurement of Stratospheric Temperatures," Quarterly Progress Report No. 107, Research Laboratory of Electronics, M.I.T., October 15, 1972, pp. 23-26.

2. J. W. Waters, "Observations of Thermal Emission from Atmospheric O_2 Lines," Quarterly Progress Report No. 107, Research Laboratory of Electronics, M.I.T., October 15, 1972, pp. 27-29.